# Noise Characteristics of an Instrumental Particle Absorbance Technique

## Stephen R. Springston and Arthur J. Sedlacek, III

*Brookhaven National Laboratory, Upton, New York, USA*

**Noise characteristics and noise reduction techniques for the particle soot absorption spectrometer (PSAP) are discussed. It is shown through elementary propagation of errors analysis and verified through simulations and by experiments that the PSAP signal noise varies as the −3/2 power of the integration time and not the assumed −1/2. It is also shown that neither simple boxcar averaging of independent absorptivity values nor the commonly used moving boxcar average allow realization of the maximum signal to noise ratio. Instead it is argued that maximal noise reduction is realized by post-processing of the raw reference and sample channel intensities. Finally the implications of these findings are demonstrated with representative field data.**

## INTRODUCTION

With the increased attention given to the role of aerosol forcing on climate change, quantification of the direct and indirect aerosol effects have become a targeted priority (Charlson et al. 1992; Chylek and Wong 1995; Hansen et al. 1997; Hansen et al. 1998; Kaufman et al. 2002; Schwartz 2004). Efforts to better quantify aerosol light absorption has spurred both the creation of new instrumentation (e.g., photoacoustic spectrometry [PAS]: Arnott et al. 2003; Arnott et al. 2000; Arnott et al. 1999; Moosmüller et al. 1997; single particle soot photometer [SP2]: Gao et al. 2007; Baumgardner et al. 2004; Stephens et al. 2003; Kok et al. 2002; photothermal interferometry [PTI]: Sedlacek 2006; Sedlacek and Lee 2007) and deployment of mature in-

strumentation, such as the particle soot absorption spectrometer (PSAP, Radiance Research, Shoreline, WA) and Aethelometer (Magee Scientific, Berkeley, CA), in new monitoring scenarios. In this article, we wish to address the latter class of instrument with respect to deployments where high precision data sets with fast temporal response are required. Improved measurement precision is required because outside of urban regions, aerosol light absorption coefficients typically range from 0–10 Mm$^{-1}$. As a case in point, a 4-y median of 1.5 Mm$^{-1}$ was measured on the ground at the ARM SGP site (Sheridan et al. 2001). However, in addition to the need for precision, aircraft-based sampling imposes stringent temporal requirements (ca. seconds) when characterizing point source plumes (Springston et al. 2005).

The PSAP is a filter-based technique (Schmid et al. 2006; Virkkula et al. 2005, Anderson et al. 2003; Anderson et al. 1999; Bond et al. 1999) where aerosols are continuously deposited onto a glass filter (e.g., Pallflex type E70.2075W) at a known flow rate and the change in the measured transmission over time is related to the particle's absorption coefficient via Beer's law. The PSAP uses the time differential of the integrated aerosol signal to calculate absorption as a function of time. Use of the difference methodology allows some noise sources such as LED output fluctuations and detector response to be greatly reduced. Additionally, the absorption coefficient is measured independently at three visible wavelengths using sequential illumination by three LEDs.

In this article, we wish to discuss both a fundamental noise issue of the PSAP with respect to averaging time, $t_{avg}$, and to examine the introduction of noise due to internal processing by the PSAP firmware. The first issue was noted during field measurements aboard an aircraft, where the background noise decreased by ~10× after changing the instrument "averaging period," signified here as $\Delta t$, from 2 to 10 s. This dramatic decrease in the noise contrasted with the widely accepted assumption that the noise in the PSAP-generated absorption coefficient is normally distributed, and thus, the noise scales proportionally to $t_{avg}^{-0.5}$ (Bond et al. 1999; Anderson et al. 1999). In those papers, $t_{avg}$ is used interchangeably with $\Delta t$ to denote both the instrument "averaging period" set from the front panel as well as the window of time used for offline (post-processing) boxcar averaging of the data. We would like to point out that the noise does not scale as

$t_{avg}^{-0.5}$ and that a significant departure from this expected dependence is borne out in simulations and experiments. In addition, because of a peculiarity in the PSAP output, boxcar averaging of the resulting data is not appropriate for this instrument. In the following discussion, we limit the definition of $t_{avg}$ to boxcar averaging in time of the absorption coefficients and $\Delta t$ to denote the averaging period as displayed on the front panel of the PSAP. We shall use these as operational definitions to assist in comparing the *relative* effects of changes in $t_{avg}$ and $\Delta t$.

As introduced above and discussed elsewhere (Schmid et al. 2006; Virkkula et al. 2005; Anderson et al. 2003; Anderson et al. 1999; Bond et al. 1999), the PSAP technique measures the particle absorption coefficient ($\sigma_{AP}$) as a function of the decrease in transmittance, $Tr$, over time as particles accumulate on the filter; that is:

$$\sigma_{AP} = \frac{A}{F\Delta t}\left(Tr_{t-\Delta t} - Tr_t\right) \qquad [1]$$

where $A$ is the filter area, $F$ is the volumetric flow rate, $Tr_t$ is the sample transmittance for the current averaging period and $Tr_{t-\Delta t}$ is the sample transmittance for the previous averaging period, $\Delta t$. The change in $Tr$ over $\Delta t$ is $\ll 1$ and therefore the simplification of $\ln Tr_{t-\Delta t}/Tr_t = Tr_{t-\Delta t} - Tr_t$ was used to derive Equation (1) from Beer's law.

The filter transmittance is calculated (Virkkula et al. 2005) for each wavelength as:

$$Tr = \frac{(\Sigma Sig/\Sigma Ref)}{(\Sigma Sig/\Sigma Ref)_{t=0}} \qquad [2]$$

where $\Sigma Sig$ and $\Sigma Ref$ are the detector outputs for the signal and reference channels summed over the same period, $\Delta t$. The reference channel includes an identical filter downstream of the sample channel and is illuminated by the same light source in order to further reduce certain common-mode noise sources such as LED output fluctuations and changes in the optical properties of the filter media. The denominator of Equation (2) normalizes the transmittance to the value of a new filter. In operation, the filter is changed when $Tr < 0.7$ (Bond et al. 1999). Using basic error propagation, the noise of the PSAP, $\delta\sigma_{AP}$, is written as a function of the noise in the transmittance.

$$\delta\sigma_{AP} = \sqrt{\Sigma\left(\frac{\partial\sigma_{AP}}{\partial x_i}\right)^2(\delta x_i)^2}$$
$$= \sqrt{\left(\frac{A}{F\Delta t}\right)^2\left((\delta Tr_{t-\Delta t})^2 + (\delta Tr_t)^2\right)} \qquad [3]$$

The noise of $Tr$ is relatively constant, i.e., $\delta Tr_{t-\Delta t} = \delta Tr_t = \delta Tr$. Assuming the noise for a given channel is dominated by shot noise, the relative noise in the intensity (and therefore for $Tr$ as well) averaged over period $\Delta t$ is, indeed, the expected

$\delta Tr \propto \Delta t^{-0.5}$. Substitution into Equation (3) yields:

$$\delta\sigma_{AP} = \frac{A\delta Tr}{F\Delta t}\sqrt{2} \propto \Delta t^{-1.5} \qquad [4]$$

which is the dependence of absorption coefficient noise on averaging period. This straightforward analysis reveals that the PSAP noise should change proportionally to the 1.5 power with respect to averaging period and not the square root as has been previously assumed (Anderson et al. 1999; Bond et al. 1999). As a consequence, the noise in the absorption coefficient measured by a PSAP (as well as by an Aethelometer and other difference measurements [Petzold and Schönlinner 2004; Petzold et al. 2002]) will increase at a much faster rate with shorter integration times as noted in the field in comparison with the noise from instruments that directly measure aerosol absorption (e.g., PAS, PTI, or SP2). This result is of fundamental importance because of the community's needs for faster time response and/or better precision from its aerosol absorption photometers. Note also that the instrument noise in absorbance as measured by the PSAP is independent of the signal magnitude. It should be pointed out that the same conclusion can also be reached by starting with the noise of the signal and reference outputs as defined in Equation (2).

Next we wish to point out that the noise characteristics of the instrument are further affected by *how* the data output is used and the instrument averaging period as controlled on the PSAP's front panel. In order to discuss this, we briefly describe how the commercial instrument produces measurement data.

An embedded microprocessor delivers output through a serial port as an ASCII character string, which is updated once per second. This output has two sections that share much redundant information albeit in different forms, however, there are some important features unique to each one. The initial section contains date, time, absorption coefficients, transmittances, flows, averaging period setting, and a status flag. Each of these values is refreshed every second. Absorption coefficients are calculated internally using the measured flow volume, a calibrated spot size, and correction factors due to scattering by the filter itself (Bond et al. 1999) as well as the change in intensities. The absorption coefficients at time $t$ are calculated from the summed intensities measured over $\Delta t$ and the summed intensities measured over the preceding $\Delta t$ interval as described in Equations (1) and (2). *This calculation is repeated and new values are output every second regardless of the instrument's $\Delta t$ setting.* Transmittances are calculated using integrated sample and reference intensities (Equation [2]) and are output with three significant figures. For calculating $\sigma_{AP}$ at a typical flow rate and filter area, a relative change in transmission of $10^{-6}$ corresponds to an apparent absorbance of ~1 Mm$^{-1}$. Thus, the transmittance values are useful as a measure of filter loading but are not reported with sufficient digital resolution to reproduce the reported $\sigma_{AP}$ values.

The second data section contains raw A-to-D intensity values as hexadecimal numbers as well as the calibration and correction factors used internally to produce the values in the first

section. However, unlike the first section's processed absorption coefficients, the raw cumulative intensities for the sample and references channels for a given wavelength are only reported once every four seconds. Whereas the first section uses a variable summation period to calculate absorption coefficients, that is, the averaging period ($\Delta t$) as set by the front panel "averaging time," the hexadecimal intensities are reported at a fixed, 4-s, summation time. In contrast to the instrument-calculated absorption coefficients that have been filtered over the averaging period, the hexadecimal intensities can only be further averaged during external post processing.

## EXPERIMENTAL

In order to quantify the noise characteristics introduced above, a combination of numerical simulations and experiments was undertaken. Aspects of the general behavior noted here have been observed in other labs (Sheridan 2007). For these experiments, a three-wavelength PSAP was employed (Radiance Research, Shoreline WA, S/N: 0020). This model is typical of units used for ground- and aircraft-based measurement campaigns. Virkkula et al. (2005) describe a prototype PSAP where the three colored LEDs are slowly cycled (6 to 60 s for a total cycle), however, as produced by Radiance and described herein, the LEDs cycle at 15 Hz, with each color (and a dark interval) having an equal duty cycle of 25%.

The noise characteristics of the PSAP were examined in three different ways. First, the effects of simulated random detector noise on instrument output were studied for three different averaging methods: (1) a boxcar average of independent data points, (2) a moving boxcar average, and (3) changing the integration (summing) period. Next the same averaging methods were applied to laboratory measurements of filtered air. Finally we demonstrate the benefits of proper averaging methods using aircraft-based measurements as an example.

The first effort involved simulating the PSAP noise characteristics as the averaging period is changed, as would be done from the instrument's front panel. For this model, Gaussian noise was added to a simulated photometric signal on a 1-second time base. The transmittance signal corresponding to an idealized square impulse of absorption coefficient was calculated using Equation (1) first rewritten as:

$$\sigma_{AP} = \frac{A Tr_t}{F \Delta t}\left(\frac{Tr_{t-\Delta t}}{Tr_t} - 1\right) \qquad [5]$$

and solving for $Tr_t$ under conditions of $Tr_t$ close to 1:

$$Tr_i = \frac{Tr_{t-\Delta t}}{(\sigma_{AP} F \Delta t / A) + 1} \qquad [6]$$

Equation (6) holds for small changes in $Tr$ over $\Delta t$. The transmittance at $t = 0$ was set to 1 and subsequent $Tr_t$ values were calculated with $\Delta t = 1$ and the ratio of F/A set to $7.1 \times 10^{-7}$ Mm/s, which is typical for the PSAP. A randomly selected value

from a Gaussian distribution with a relative standard deviation of $2.5 \times 10^{-6}$ was added to each transmittance value to simulate shot noise at the detector. This fraction was chosen to approximate the noise observed with the PSAP. Then the absorption coefficient signal containing noise was recalculated with varying values of $\Delta t$ using Equation (1).

For laboratory experiments, HEPA-filtered air was sampled at various instrument averaging periods ($\Delta t = 2, 3, 4, 5, 12, \ldots, 30$ s). The resulting data, output every second, were parsed to produce a record of instrument-calculated absorption coefficients. Noise in this signal changed with $\Delta t$. In contrast, the hexadecimal portion of the output string (which contains the ongoing summation of the reference and sample channel intensities) is unaffected by the averaging period setting and was further parsed into individual components. These values were processed externally into another record of absorption coefficients. Because the hexadecimal intensity data for each wavelength is only delivered once every four seconds, the externally calculated absorption coefficients are only available at a rate of 0.25 Hz. By changing the period over which the intensity ratios are calculated, the effect of changing the front-panel averaging period could be simulated but only by multiples of 4 seconds (i.e., 4, 8, 12, ..., 128 s). The processing algorithm was confirmed for both ambient and filtered air by comparing instrument-calculated and externally-processed results. External processing exactly replicated the instrument's internal processing at $\Delta t = 4$ and 12 s with one important difference as discussed later.

Finally, ambient measurement data recorded during the 2006 Megacities Aerosol eXperiment- Mexico (MAX-Mex) program (ftp://ftp.asd.bnl.gov/pub/ASP%20Field%20Programs/2006MAXMex/) were reprocessed externally and the results compared with a simple boxcar averaging scheme of the instrument output that is typically used in the community.

## Averaging Methods

In general, the time constant of measurement data is determined by the time constants of individual elements in the system including inlet mixing and diffusion, cell volume and the time response of the electronics. It is common practice to record data at the highest practical response speed and then average the data during post processing in order to reduce noise. When performed with an absolute technique (nephelometry, thermometry, etc.) such averaging reduces the noise proportional to the square root of the averaging time. However, since the PSAP measures the relative change of absorbance over time, the change in noise with averaging time is different and depends on the application of the averaging filters.

Three different averaging methods were applied to data from the PSAP. Case I refers to a boxcar average of width $t_{avg}$ applied to *independent* absorptivity values. Case II refers to a boxcar average of width $t_{avg}$ applied at 1-s increments to the absorptivity values produced every 1-s by the instrument. Case II represents the typical averaging method for smoothing data. Finally, in Case III the averaging period, $\Delta t$, of Equation (1)

is varied. The instrument firmware averages data using Case III as controlled by the front panel setting of $\Delta t$ (denoted as Case IIIA in the Results section). The same algorithm can also be applied in post processing of the hexadecimal data (denoted as Case IIIB). In each case, noise was calculated as the standard deviation of a time series of data for a constant signal. The three cases were compared by measuring the change in noise as $t_{avg}$ and $\Delta t$ were varied.

## RESULTS AND DISCUSSION

### Simulation Data

Figure 1A shows an idealized input signal and the absorbance signal with white Gaussian noise added to the transmittance (signal + noise). The lower traces illustrate the effects of each averaging method. Case I shows an 8-s boxcar filter applied



FIG. 1. (a) Simulation of PSAP processing. From top: Idealized square input signal with a width of 32 s and a height of 5 Mm$^{-1}$; Signal with white Gaussian noise superimposed on the transmittance. Magnitude of noise is $2.5 \times 10^{-6}$ times the transmittance (note different ordinate scale); Noisy signal processed with Case I ($\bullet$) and $t_{avg} = 8$ s; Noisy signal processed with Case II ($\blacksquare$) and $t_{avg} = 8$ s; Noisy signal processed with Case III ($\blacktriangle$) and $t = 8$ s. (b) Log noise as a function of log averaging/summation time with linear regression fit. Case I, slope $= -0.5$, Case II, slope $= -1.0$, Case III, slope $= -1.5$.

to *independent* absorptivity values. Case II shows the signal averaged with an 8-s running boxcar filter and Case III shows the same transmittance record processed with an 8-s summation time. Visually, Case III shows the best fidelity to the input signal and the lowest noise.

The standard deviation of the baseline was calculated for each case and averaging period. The log of the standard deviation plotted *versus* the log of the averaging period is shown in Figure 1(b). The slopes of these lines correspond to the exponents relating the noise to averaging time as developed for Case III in Equation (4). For independent absorptivity values, the slope is $-0.5$ as is typical of an absolute (non-integrating) technique. Case II illustrates the effect of averaging the output data of the PSAP where the noise decreases proportionally with the averaging time (exponent $= -1$). The slope of $-1.5$ in Case III supports the derivation of Equation (4) relating the signal noise to the averaging period.

### Data from HEPA-Filtered Air

The analysis of results refer only to the blue channel of the PSAP but is applicable to the other two wavelengths as well. Inspection of the power spectrum of raw transmittance values (available in the hexadecimal output at 0.25 Hz) showed the characteristics of white noise. In processing the hexadecimal data, the same transmission correction function built into the firmware (Bond et al. 1999) was applied to all absorption coefficients calculated externally (K0 $= 1.0796$ and K1 $= 0.71$). This empirical correction accounts for absorption by the filter medium and response nonlinearities as material is deposited onto the filter.

The PSAP firmware delivers calculated absorption coefficients in the ASCII output string with a fixed digital resolution of 0.1 Mm$^{-1}$. Thus, the resolution precision is limited to $\pm 0.05$ Mm$^{-1}$ regardless of the averaging period. However, the output resolution is further limited. Using HEPA-filtered air as a proxy for low signal conditions, Figure 2 shows a histogram of output values plotted with a bin width of 0.1 Mm$^{-1}$, which corresponds to the resolution of the PSAP's ASCII output. There is a clear over abundance of values at 0.0 and deficits of values at 0.2, 0.1, 0.1, and 0.2 Mm$^{-1}$. This behavior is present over the entire range of output values and is presumably caused by internal roundoff or truncation errors in the firmware of the embedded microprocessor. *Longer instrument averaging periods do not reduce this roundoff behavior.* We note that the overall shape of the distribution in Figure 2 is Gaussian which accounts for the linearity in the cumulative, log-probability distributions reported by Anderson et al. (2003) and interpreted therein as evidence for normally distributed noise. In addition to digitization and truncation limitations, we now show how the noise is affected by the interdependence of adjacent measurements.

The noise component of each data point produced by the PSAP is highly anti-correlated with its adjacent neighbors. As illustrated in Figure 3, the autocorrelation of the 1-s ASCII absorptivity signal (solid line) shows that points both 2 s before and 2 s after tend to diverge from the mean in the opposite
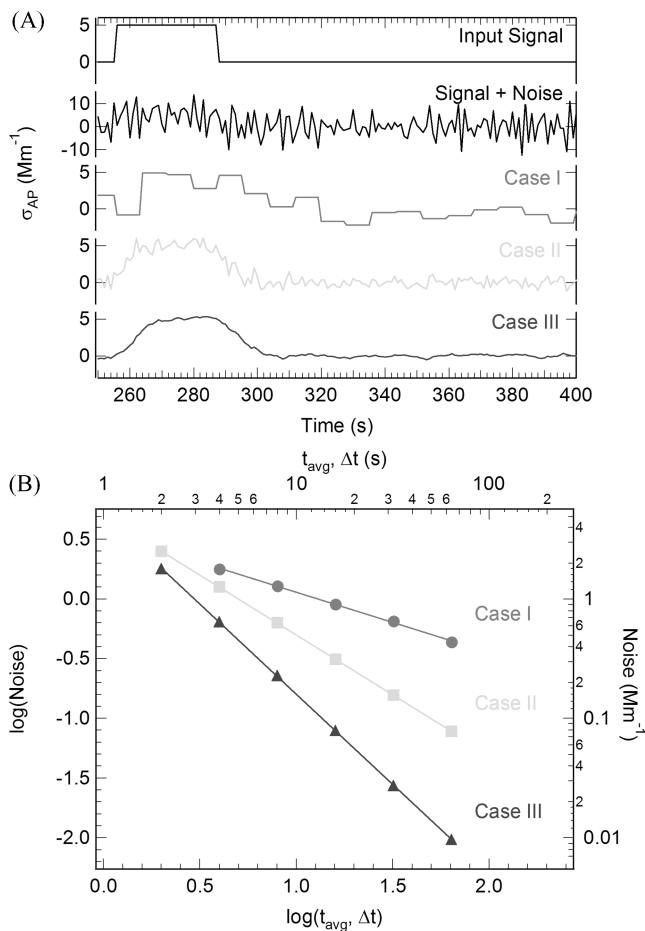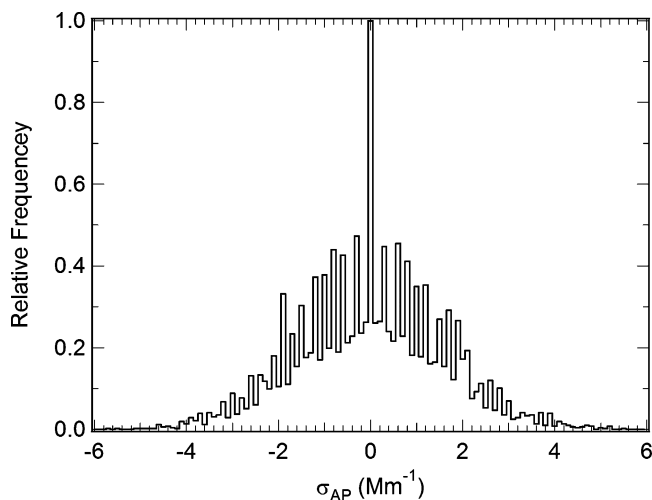
FIG. 2. Histogram of PSAP output values (blue channel, N = 7244) while sampling HEPA filtered air. Absorption coefficient measured with instrument t = 2 s.

direction. In contrast, if the autocorrelation is done using only every fourth point (dashed line), there is no evidence of interdependence between adjacent points. We attribute this behavior to the measurement technique itself, $Tr_t$ is compared with $Tr_{t-\Delta t}$. Thus, any noise excursion in a single transmittance measurement point (or average) tends to manifests itself in the opposite direction in the succeeding point (or average). For the sole purpose of noise analysis, it is necessary to work with independent data points. *As presently configured, the shortest averaging time setting for the commercial PSAP is 2 s which produces an independent point only once every 4 seconds.* Note that this behavior applies not only to the PSAP, but is inherent in taking the differential of an integrated sample (e.g., Aethelometer). We also
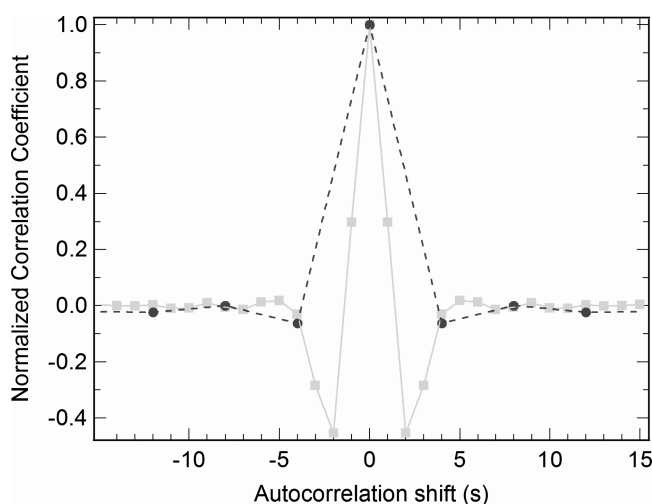


FIG. 3. Autocorrelation of PSAP output values (blue channel) while sampling HEPA filtered air. (■) Data as output every 1-s by the PSAP, (●) t = 2 s. The same data taking only every fourth point. These data are independent.
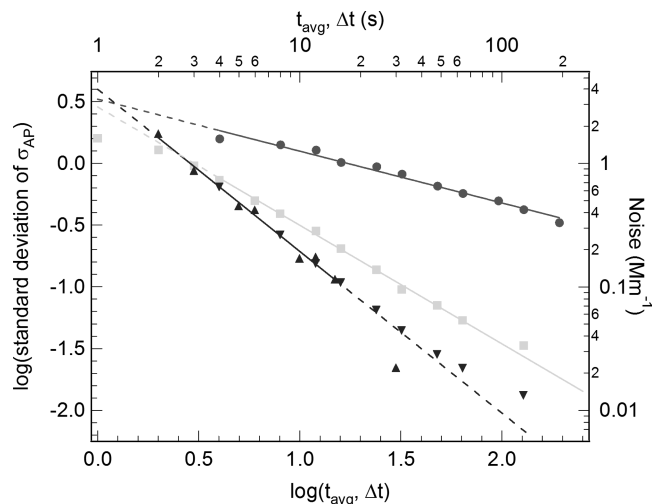


FIG. 4. PSAP measurement data (blue channel) of HEPA filtered air. Log noise as a function of log averaging/summation time with linear regression fit. Compare with Figure 1(b). Case I (●), slope = −0.42, Case II (■), slope = −0.96, Case IIIA (▲), Case IIIB (▼), slope = −1.31. Solid lines are linear regression over the points used. Broken lines are extrapolations. Unused points are explained in the text.

observe the same anti-correlation of points calculated with external processing.

The same three averaging methods described above were applied to measurement data produced by the PSAP as it sampled particle-free air. The differences between the three cases and their effects on baseline noise as a function of averaging time are shown in Figure 4. For Cases I and II, the experimental results agree well with the simulation results of Figure 1b. Case III has been further divided to distinguish between instrument-calculated (Case IIIA) and externally processed (Case IIIB) values. In both examples of Case III, the standard deviation of the signal is observed to vary proportional to $\Delta t^{-1.31}$. This is somewhat greater than the $\Delta t^{-1.5}$ derived in the introduction and observed with simulated noise, but is significantly different than the $t_{avg}^{-0.5}$ reported in the literature (Bond et al. 1999 and Anderson et al. 1999). Note that $\Delta t$ is distinct from $t_{avg}$ in that $\Delta t$ is in effect applied twice in processing: first as the summation interval for intensities (Equation [2]) and second as the time interval for change in intensity (Equation [1]).

Several points which were excluded from the regression lines shown in Figure 4 are worth noting. Even though the PSAP delivers a data point every second, the minimum instrument averaging period is 2 s. Thus the point for Case II at $t_{avg} = 1$ s refers to the noise of the instrument produced signal which is already averaged by the internal processing. At $\Delta t$ greater than 15 s, the Case IIIA values of standard deviation are less than the digitization resolution limit of ±0.05 Mm$^{-1}$ and the points deviate negatively. The limited resolution and the internal truncation/roundoff error mean long instrument averaging periods cannot be used to make absorbance measurements with precision finer than ∼0.2 Mm$^{-1}$. On the other hand, external

processing (Case IIIB) is not limited by roundoff errors and averaging periods can be extended greater than 100 seconds. The positive deviations from the regression line for Case IIIB at $\Delta t > 32$ s are explained by residual signal and instrument drift. For $\Delta t > 100$ s, the noise appears to approach $0.01$ Mm$^{-1}$, which may constitute the limit of detection. Therefore, Case IIIB is the recommended method for averaging data when a precision better than $\sim 0.2$ Mm$^{-1}$ is necessary. However, Case IIIB should not be used when response time is at a premium, instead it is advised that the instrument-calculated absorptivities be used with $\Delta t = 2$ seconds (Case IIIA).

## Averaging of Ambient Measurement Data

PSAP data taken during aircraft-based sampling were recorded with an instrument averaging period of 2 seconds. The raw intensities were also recorded. These data were averaged using Case II and Case III methods. The original recorded data and the results of averaging are shown in Figure 5. Also included are the results from an integrating nephelometer (Model 3560,
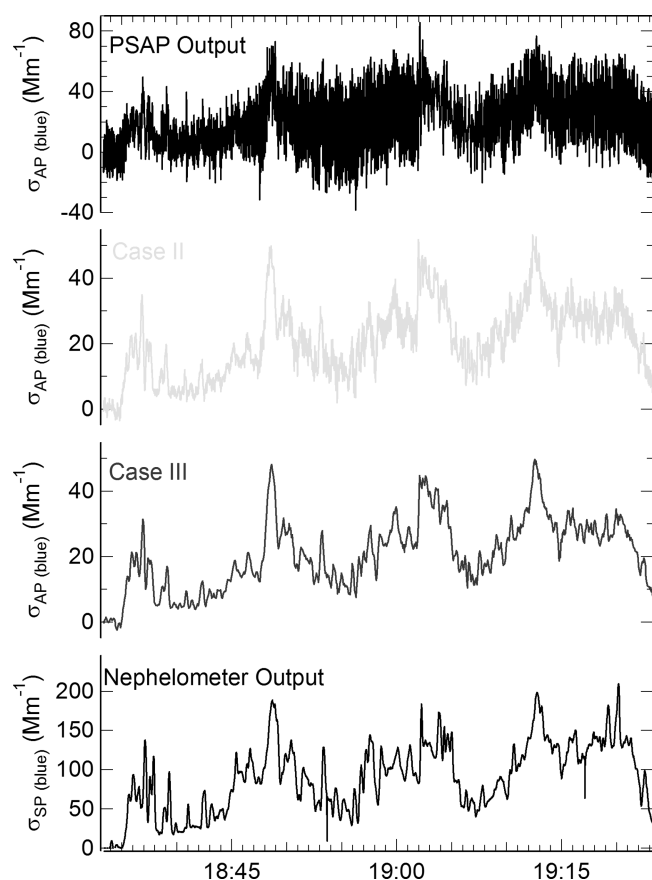


FIG. 5. PSAP measurement data (blue channel) during MAX-MEX '06. From the top: PSAP output as recorded with t = 2 s; Case II, top trace subjected to a running boxcar average, tavg = 12 s; Case III, hexadecimal intensities used to calculate absorption coefficient with t = 12 s; Nephelometer data (blue channel) from the same period showing features only apparent on the PSAP data processed with Case III.

TSI, Inc., St. Paul, MN). The reduction in PSAP noise with averaging is evident when the instrument produced signal ($\Delta t = 2$ s) is averaged by a 12-s boxcar using Case II and an even greater reduction is obtained by independently reprocessing the raw intensity data with $\Delta t = 12$ s (Case III). For direct comparison, these data were not corrected for aerosol scattering as that correction is well-known and is not the focus of this article.

## Instrument Time Response

This work has focused on instrument noise. Clearly signal averaging affects the instrument time response. We have not completed tests to measure the true instrument response time but for $\Delta t$ values greater than $\sim 10$ s, we confirm the response time approximates $\Delta t$.

## Flow Response

As a caution, we note that the PSAP firmware calculates the mass flow rate from the sensor output using a two segment spline. We have observed that this sensor (Honeywell AWM5101VN) responds quadratically to flow. With the three flow parameters entered correctly at the front panel, at flows near the recommended 1 SLPM, the PSAP tested under reported the true flow by $\sim 10\%$ and thus overstated the absorption coefficients by the same amount. A quadratic calibration curve is recommended to convert the sensor voltage to mass flow rate.

## CONCLUSIONS

Elementary propagation of errors analysis shows the noise of the PSAP technique should vary as $\Delta t^{-1.5}$ and not the previously assumed $\Delta t^{-0.5}$. This behavior is confirmed by simulated data. Experimental tests confirm that instrument averaging reduces the noise at a rate proportional to $\sim \Delta t^{-1.3}$. The instrument-calculated absorptivities suffer from limited digital resolution as well as internal roundoff errors. Instrument calculated absorptivities are further limited by the instrument averaging period setting. If the averaging setting is set too long, the faster portion of the signal ($<4$s) is lost and cannot be recovered. If it is set too short, the instrument-calculated absorptivities cannot be simply averaged (Case I and II) to reduce the noise as effectively as other methods. For the best performance, the instrument should always be operated at the shortest (2-s) averaging period. Independent values of data are then reported every 4 seconds with a standard deviation of $\sim 1.6$ Mm$^{-1}$ (Case IIIA). Where better precision is desired at the expense of time response, the hexadecimal values should be used to calculate absorptivities. Case IIIB can be applied post collection, does not suffer from digital resolution limitations, roundoff or truncation errors, and is independent of the instrument averaging period setting.

Case IIIB is only limited by the frequency of the hexadecimal output. Simple averaging of the instrument-calculated absorptivities should never be done. These recommendations are summarized in Table 1.

TABLE 1

| Measurement Goal | Use | Noise | Limitations |
|---|---|---|---|
| Fastest Response | ASCII Output $\Delta t = 2$ s | $\delta\sigma_{AP} \sim 1.6$ Mm$^{-1}$ | Precision limited cannot be averaged |
| Greatest Signal/Noise | Hex Output $\Delta t >= 4$ s | $\delta\sigma_{AP} = 10^{(0.60-1.31*log(\Delta t))}$ | Loss of fastest signal |

Future instruments based on the integrating filter method should incorporate changes to the internal firmware. These changes include higher numerical precision in the calculations and reported values. Reporting of all instrument parameters for every wavelength at one hertz is clearly justified. Because of the $\Delta t^{-1.5}$ relationship to noise derived in Equation (4), at speeds commensurate with aircraft-based sampling the integrating filter technique is unsuitable for measuring the spatial variability of aerosols at low loadings. For faster response a direct measurement of particle absorbance is needed (PAS, SP2, and PTI).

## REFERENCES

Anderson, T. L., Masonis, S. H., Covert, D. S., Ahlquist, N. C., Howell, S. G., Clark, A. D., and McNaughton, C. S. (2003). Variability of Aerosol Optical Properties Derived from In Situ Aircraft Measurements During ACE-Asia, *J. Geophys. Res.* 108(D23): 8647.

Anderson, T. L., Covert, D. S., Wheeler, J. D., Harris, J. M., Perry, K. D., Trost, B. E., Jaffe, D. J., and Ogren, J. A. (1999). Aerosol Backscatter Fraction and Single Scattering Albedo: Measured Values and Uncertainities at a Coastal Station in the Pacific Northwest, *J. Geophys. Res.* 104: 26793–26807.

Arnott, W. P., Moosmüller, H., Sheridan, P. J., Ogren, J. A., Raspet, R., Slaton, W. V., Hand, J. L., Kreidenweis, S. M., and Collett Jr., J. L. (2003). Photoacoustic and Filter-based Ambient Aerosol Light Absorption Measurements: Instrument Comparisons and the Role of Humidity, *J. Geophys. Res.* 108(D1): 4034, doi: 10.1029/2002JD002165.

Arnott, W. P., Moosmüller, H., and Walker, J. W. (2000). Nitrogen Dioxide and Kerosene-Flame Soot Calibration of Photoacoustic Instruments for Measurement of Light Absorption by Aerosols, *Rev. Sci. Instru.* 71: 4545.

Arnott, W. P., Moosmüller, H., Rogers, C. F., Jin, T., and Bruch, R. (1999). Photoacoustic Spectrometer for Measuring Light Absorption by Aerosol: Instrument Description, *Atmos. Env.* 33: 2845.

Baumgardner, D., Kok, G., and Raga, G. (2004). Warming of the Arctic Lower Stratosphere by Light Absorbing Particles. *Geophys. Res. Lett.* 31: L06117.

Bond, T. C., Anderson, T. L., and Campbell, D. (1999). Calibration and Intercomparison of Filter-Based Measurements of Visible Light Absorption by Aerosols, *Aerosol Sci. Technol.* 30: 582–600.

Charlson, R. J., Schwartz, S. E., Hales, J. M., Cess, R. D., Coakley, J. A., Hansen, J. E., and Hofmann, D. J. (1992). Climate Forcing by Anthropogenic Aerosols, *Science* 255: 423.

Chylek, P., and Wong, J. (1995). Effect of Absorbing Aerosols on Global Radiation Budget, *Geophys. Res. Lett.* 22: 929.

Gao, R. S., Schwarz, J. P., Kelly, K. K., Fahey, D. W., Watts, L. A., Thompson, T. L., Spackman, J. R., Slowik, J. G., Cross, W. E. S., Han, J.-H., Davidovits, P., Onasch, T. B., and Worsnop, D. R. (2007). A Novel Method for Estimating Light-Scattering Properties of Soot Aerosols using a Modified Single-Particle Soot Photometer, *Aerosol Sci. Technol.* 41: 125–135.

Hansen, J. E., Sato, J., and Redy, R. (1997). Radiative Forcing and Climate Response, *J. Geophys. Res.* 102: 6831.

Hansen, J. E., Sato, J., Lacis, A., Ruedy, R., Tegen, I., and Matthews, E. (1998). Climate Forcing in the Industrial Era, *Proc. Natl. Acad. Sci.* 95: 12753.

Kaufman, Y. J., Tanré, D., Holben, B. N., Mattoo, S., Remer, L. A., Eck, T. F., Vaughan, J., and Chetenet, B. (2002). Aerosol Radiative Impact on Spectral Solar Flux at the Surface, Derived from Principal-Plane Sky Measurements, *J. Atmos. Sci.* 59: 635.

Kok, G. L., Baumgardner, D., Spuler, S. (2002). A Single Particle Soot Photometer for the Measurement of Aerosol Black Carbon, American Geophysical Union, Fall Meeting 2002, abstract #A12G-02.

Moosmüller, H., Arnott, W. P., and Roger, C. F. (1997). Methods for Real-Time, In Situ Measurement of Aerosol Light Absorption, *J. Air and Waste Manage. Assoc.* 47: 157.

Petzold, A. and M. Schönlinner (2004). Multi-Angle Absorption Photometry—A New Method for the Measurement of Aerosol Light Absorption and Atmospheric Black Carbon, *J. Aero. Sci.* 35: 421.

Petzold, A., Kramer, H., and Schönlinner, M. (2002). Continuous Measurement of Atmospheric Black Carbon Using a Multi-Angle Absorption Photometer, *Env. Sci. Pollut. Res.* 4: 78.

Schmid, O., Artaxo, P., Arnott, W. P., Chand, D., Gatti, L. V., Frank, G. P., Hoffer, A., Schnaiter, M., and Andreae, M. O. (2006). Spectral Light Absorption by Ambient Aerosols Influenced by Biomass Burning in the Amazon Basin. I: Comparison and Field Calibration of Absorption Measurement Techniques, *Atmos. Chem. Phys.* 6: 3443.

Schwartz, S. E. (2004). Uncertainty Requirements in Radiative Forcing of Climate Change, *Air & Waste Mange. Assoc.* 54: 1351–1359.

Sedlacek, A. J. (2006). Real-Time Detection of Ambient Aerosols Using Photothermal Interferometry: Folded Jamin Interferometer, *Rev. Sci. Instrum.* 77: 064903.

Sedlacek, A. J. and Lee, J. (2007). Photothermal Interferometric Aerosol Absorption Spectrometry, Aerosol Sci. Technol. (in press).

Sheridan, P. J. (2007). Personal Communication.

Sheridan, P. J., Delene, D. J., and Ogren, J. A. (2001). Four Years of Continuous Surface Aerosol Measurements from the Department of Energy's Atmospheric Radiation Measurement Program Southern Great Plains Cloud and Radiation Testbed Site, *J. Geophys. Res.* 106: 20735–20747.

Stephens, M., Turner, N., and Sandberg, J. (2003). Particle Identification by Laser-Induced Incandescence in a Solid-State Laser Cavity, *Applied Optics* 42(19): 3726–3736.

Springston, S. R., Kleinman, L. I., Brechtel, F., Lee, Y.-N., Nunnermacker, L. J., and Wang, J. (2005). Chemical Evolution of an Isolated Power Plant Plume During the TexAQS 2000 Study, *Atmos. Environ.* 39: 3431.

Virkkula, A., Ahlquist, N. C., Covert, D. S., Arnott, W. P., Sheridan, P. J., Quinn, P. K., and Coffman, D. J. (2005). Modification, Calibration and a Field Test of an Instrument for Measuring Light Absorption by Particles, *Aerosol Sci. Technol.* 39: 68–83.